Impact of micro-computed tomography reconstruction protocols on bone microarchitecture analysis

Eduarda Helena Leandro Nascimento, DDS, MD,[a] Hugo Gaêta-Araujo, DDS, MD,[a] Danieli M. Brasil, DDS, MD, PhD,[a] Daniela Verardi Madlum, DDS,[a] Deborah Q. Freitas, DDS, MD, PhD,[a] Frascisco Haiter-Neto, DDS, MD, PhD,[a] and Christiano Oliveira-Santos, DDS, MD, PhD[b]

Objective. The aim of this study was to assess the influence of reconstruction protocols of micro-computed tomography (micro-CT) images on analyses of bone microarchitecture.

Study Design. Micro-CT images of the maxillae of 5 Wistar rats were reconstructed with different protocols by varying the levels of the following tools: smoothing filter (SF; 2−6); ring artifact correction (RAC; 5−15); and beam hardening correction (BHC; 15%−60%). A control protocol (P0; without any correction tool) and a standard protocol (SP; according to the manufacturer's recommendation: SF = 2; RAC = 5; BHC = 45%) were also obtained. For each protocol, 8 bone microarchitecture parameters were calculated (bone volume/total volume [BV/TV], bone surface/total volume [BS/TV], trabecular number [Tb.N], trabecular thickness [Tb.Th], trabecular separation [Tb.Sp], degree of anisotropy [DA], connectivity density [Conn.D], and total porosity [Po-tot]) by using CTAn software. Test protocols were compared with the SP by using 1-way analysis of variance and the Dunnet post hoc test ($\alpha = 0.05$).

Results. An inverse relationship was observed between BHC tool levels and all microarchitecture parameters except BV/TV and Tb.Th. The combination of BHC and SF significantly influenced all microarchitecture parameters except for DA, for which all protocols were similar to the SP ($P > .05$).

Conclusions. Calculation of bone microarchitecture parameters is influenced by the applied levels of artifact correction tools, mainly BHC and SF. It is necessary to standardize such tool levels for correct data interpretation. (Oral Surg Oral Med Oral Pathol Oral Radiol 2019;128:411−417)

Micro-computed tomography (micro-CT) is a nondestructive high-resolution method for analyzing 3-dimensional (3-D) structures. It is currently considered the reference standard for the analysis of bone morphology and microarchitecture.[1] However, although several studies have shown that micro-CT images present high correlation with histologic analysis and excellent accuracy and reproducibility,[1−3] the polychromatic characteristic of the X-ray beam generates beam-hardening effects, which may cause errors during data processing and compromise the precision of data analysis.[4] In addition, the noise inherent in the process of image formation and defects in sensor pixels (which can generate ring artifacts) contribute to a decrease in image quality.

To overcome these limitations and improve the quality of the image, micro-CT systems generally offer artifact correction tools to be used during the image reconstruction process.[5] The smoothing filter, ring artifact correction, and beam-hardening correction are among the most commonly used tools for this purpose.[6] The smoothing filter (SF) and the ring artifact correction (RAC) tools usually apply different smothing kernels and median filters through polar or cartesian coordinates, respectively, whereas the beam-hardening correction (BHC) tool works by linearization of the image pixel value discrepancies.[7,8]

Although micro-CT is a widely used method for the quantification of bone microarchitecture in several fields of medicine and dentistry,[9,10] research on the technical parameters of micro-CT image reconstruction and how they could influence the data related to bone microarchitecture analysis is lacking. Such knowledge would allow for better interpretation of the results of and the methodologic differences among studies and help highlight the importance of standardizing such parameters to obtain reliable and reproducible evaluations with the use of micro-CT.

Therefore, the purpose of this study was to evaluate the influence of reconstruction parameters of micro-CT images on the analyses of bone microarchitecture.

Statement of Clinical Relevance

Reconstruction protocols of micro-computed tomography images affect bone microarchitecture analysis, especially the beam hardening correction tool and the smoothing filter. Standardization and clear specification of these algorithms in future studies are necessary for correct interpretation and comparisons of results.

[a]Department of Oral Diagnosis, Division of Oral Radiology, Piracicaba Dental School, University of Campinas (UNICAMP), Piracicaba, São Paulo, Brazil.
[b]Department of Stomatology, Public Health, Forensic Dentistry, Division of Oral Radiology, School of Dentistry of Ribeirao Preto, University of Sao Paulo, São Paulo, Brazil.
Received for publication Jan 23, 2019; returned for revision May 3, 2019; accepted for publication May 13, 2019.

2212-4403/$-see front matter
https://doi.org/10.1016/j.oooo.2019.05.001

MATERIALS AND METHOD

Sample description and micro-CT image acquisition

This study received exemption from the Animal Use Ethics Committee because the sample stemmed from a previously approved study (protocol #3344-1/2014). The sample was composed of the maxillae of 5 Wistar rats. Each maxilla was individually scanned in a Sky-Scan 1174 micro-CT unit (Bruker, Konitch, Belgium), with settings as follows: 0.5 mm Al filter, 50 kV, 800 μA, pixel size 10.2 μm, 0.5-degree rotation step, 180-degree rotation, 2 frames on average, and scan time of 36 minutes. A single oral radiologist with 6 years of experience in micro-CT imaging performed all procedures related to scanning, image reconstruction, and analysis, as well as data tabulation.

Reconstruction parameters

Initially, a reconstruction protocol without the application of any of the artifact correction tools was carried out for each maxilla to establish a control sample (P0). For the other reconstructions, variations of 3 different artifact correction tools were applied: SF, RAC, and BHC. The standard protocol (SP) consisted of reconstructions according to the parameters for artifact reduction levels for rat bone, as recommended by the manufacturer (SF = 2; RAC = 5; BHC = 45%). Thirty-five additional protocols were applied for each maxilla by combining these parameters (varying SF from 2 to 6, RAC from 5 to 15, and BHC from 15% to 60%) The combination of tools in each protocol is shown in the first column ("Protocols") of Tables I and II. Thus, there were, in total, 37 micro-CT reconstruction protocols for each of the 5 maxillae (Figure 1).

Bone microarchitecture analysis

Images were imported into the CTAn software (Bruker, Konitch, Belgium) for bone microarchitecture analysis. A volume of interest of 5 mm diameter and 100-slice thickness was determined for each maxilla and applied to all reconstructions. Bone volume fraction (bone volume/total volume [BV/TV]), surface density (bone surface/total volume [BS/TV]), trabecular number (Tb.N), trabecular thickness (Tb.Th), trabecular separation (Tb.Sp), degree of anisotropy (DA), connectivity density (Conn.D), and total porosity (Po-tot) were obtained.[11] Table III provides an overview of the bone microarchitecture parameters studied. All parameters were calculated with 3-D integrated analysis of all objects in the volume of interest, except for BV/TV and BS/TV, which were calculated with 2-dimensional (2-D) integrated analysis, and Conn.D, which was calculated with 2-D individual analysis of all objects in the region of interest.

Statistical analysis

Mean values of the bone microarchitecture parameters were calculated. One-way analysis of variance with the Dunnet post hoc test was used to compare bone microarchitecture parameters of each experimental reconstruction protocol (P0 to P35) with the SP. The analyses were performed by using SPSS software v. 24.0 (SPSS Inc., Chicago, IL), and the level of significance was set at $P < .05$ ($\alpha = 5\%$).

RESULTS

Table I shows the mean and standard deviation (SD) values of BV/TV, BS/TV, Tb.N, Tb.Th, and Tb.Sp. Table II provides the values of DA, Conn.D, and total porosity. Different RAC levels had no significant influence on the analysis of any bone microarchitecture parameters. SF and BHC had the greatest effects on micro-CT reconstruction of the images. In general, an inverse relationship was observed between BHC tool levels and the microarchitecture parameters evaluated, except for BV/TV and Tb.Th; these values increased as this tool level was increased. Protocols 6 and 10 did not differ from SP in any of the microarchitecture parameters.

For BV/TV, except for the protocols P6, P10, P13, P17, P21, P24, P25, P28, P29, P32, and P33, all protocols were statistically different from SP ($P < .05$). In other words, when SF was set at 2 and BHC at 45%, BV/TV values remained similar to those in the SP. Likewise, among reconstruction protocols with SF of 4 and BHC of 30%, and SF of 6 and BHC of 15% or 30%, BV/TV values were similar to those in the SP ($P > .05$) (see Table I).

For BS/TV, P0 and protocols combining SF of 2 and BHC of 30% or 60%, and SF of 4 or 6 and BHC of 30%, 45% or 60%, were statistically different from the SP ($P < .05$). With all other protocols, BS/TV did not differ significantly from that in the SP ($P > .05$) (see Table I).

For Tb.N, P0, P14, P15, P18, P19, P22, P23, and all protocols with SF of 6 (regardless of RAC or BHC levels) were statistically different from SP ($P < .05$), which means that when setting SF at 2 and any value of BHC, or SF at 4 and BHC at 15% or 30%, Tb.N produced values that were similar to SP (see Table I).

For Tb.Th, P0 and protocols with SF of 2 and BHC less than 45%, SF of 4 and BHC of 60%, and SF of 6 and BHC greater than 15%, values were statistically different from SP ($P < .05$). Similar to the BV/TV results, when SF was 2 and BHC was set at 45%, BS/TV and Tb.Th values were not different from those in the SP. However, when SF was 4 or 6 combined with a BHC of 15%, BS/TV and Tb.Th remained similar to the values in the SP (see Table I).

Table I. Mean values (SD) of BV/TV, BS/TV, Tb.N, Tb.Th, and Tb.Sp for each protocol (SP and P0 to P35)

Protocols (SF-RAC-BHC)	*Microarchitecture parameters – Mean (SD)*				
	BV/TV	*BS/TV*	*Tb.N*	*Tb.Th*	*Tb.Sp*
SP (2-5-45)	91.05 (6.10)	14.90 (1.31)	4.32 (0.63)	0.21 (0.03)	0.070 (0.02)
P0 (0-0-0)	45.51 (4.21)*	57.06 (4.18)*	11.56 (0.61)*	0.04 (0.00)*	0.059 (0.01)
P1 (2-5-15)	78.05 (7.36)*	18.94 (1.35)	5.52 (0.83)	0.14 (0.02)*	0.081 (0.02)*
P2 (2-5-30)	87.08 (7.36)*	16.30 (1.31)*	4.65 (0.63)	0.19 (0.03)*	0.075 (0.02)*
P3 (2-5-60)	93.20 (4.08)*	14.18 (1.24)*	4.04 (0.60)	0.23 (0.04)	0.066 (0.01)
P4 (2-10-15)	78.06 (7.35)*	18.95 (1.39)	5.53 (0.84)	0.14 (0.02)*	0.081 (0.02)*
P5 (2-10-30)	87.12 (6.10)*	16.29 (1.32)*	4.68 (0.61)	0.19 (0.03)*	0.075 (0.02)*
P6 (2-10-45)	91.09 (4.89)	14.89 (1.31)	4.32 (0.59)	0.21 (0.03)	0.080 (0.02)
P7 (2-10-60)	93.25 (4.08)*	14.16 (1.23)*	4.04 (0.60)	0.24 (0.04)	0.066 (0.02)*
P8 (2-15-15)	78.05 (7.31)*	18.98 (1.45)	5.54 (0.87)	0.14 (0.02)*	0.081 (0.02)*
P9 (2-15-30)	87.14 (6.10)*	16.28 (1.30)*	4.68 (0.61)	0.19 (0.03)*	0.075 (0.02)*
P10 (2-15-45)	91.12 (4.89)	15.61 (2.08)	4.32 (0.59)	0.21 (0.04)	0.070 (0.02)
P11 (2-15-60)	93.28 (4.06)*	14.29 (1.26)*	4.03 (0.60)	0.24 (0.04)	0.066 (0.02)*
P12 (4-5-15)	80.05 (8.70)*	15.30 (1.25)	3.01 (1.68)	0.20 (0.04)	0.096 (0.02)*
P13 (4-5-30)	89.37 (6.21)	13.84 (1.03)*	3.64 (0.76)	0.25 (0.06)	0.086 (0.02)*
P14 (4-5-45)	93.16 (4.60)*	12.98 (0.84)*	3.43 (0.72)*	0.28 (0.07)	0.081 (0.02)
P15 (4-5-60)	95.11 (3.63)*	12.43 (0.71)*	3.16 (0.65)*	0.31 (0.07)*	0.077 (0.02)
P16 (4-10-15)	80.08 (8.71)*	15.29 (1.28)	4.01 (0.71)	0.20 (0.03)	0.096 (0.02)*
P17 (4-10-30)	89.42 (6.22)	13.83 (1.03)*	3.63 (0.75)	0.26 (0.06)	0.086 (0.02)*
P18 (4-10-45)	93.20 (4.60)*	12.97 (0.84)*	3.41 (0.71)*	0.28 (0.07)	0.081 (0.02)
P19 (4-10-60)	95.13 (3.61)*	12.41 (0.71)*	3.15 (0.64)*	0.31 (0.07)*	0.077 (0.02)
P20 (4-15-15)	80.08 (8.70)*	15.30 (1.31)	4.01 (0.72)	0.20 (0.03)	0.096 (0.02)*
P21 (4-15-30)	89.44 (6.23)	13.82 (1.02)*	3.62 (0.75)	0.26 (0.06)	0.086 (0.02)*
P22 (4-15-45)	93.23 (4.58)*	12.96 (0.84)*	3.41 (0.72)*	0.28 (0.07)	0.081 (0.02)
P23 (4-15-60)	95.15 (3.61)*	12.40 (0.70)*	3.14 (0.64)*	0.31 (0.07)*	0.077 (0.02)
P24 (6-5-15)	81.53 (9.79)	13.71 (1.44)	3.45 (0.83)*	0.25 (0.06)	0.104 (0.03)
P25 (6-5-30)	91.45 (6.12)	12.81 (0.87)*	3.12 (0.72)*	0.30 (0.07)*	0.091 (0.02)
P26 (6-5-45)	95.04 (4.02)*	12.04 (0.65)*	2.89 (0.37)*	0.33 (0.05)*	0.085 (0.03)
P27 (6-5-60)	96.61 (3.01)*	11.62 (0.49)*	2.71 (0.21)*	0.36 (0.04)*	0.079 (0.03)
P28 (6-10-15)	81.58 (9.81)	13.70 (1.47)	3.44 (0.83)*	0.25 (0.06)	0.104 (0.03)
P29 (6-10-30)	91.48 (6.12)	12.81 (0.86)*	3.13 (0.72)*	0.30 (0.07)*	0.091 (0.02)
P30 (6-10-45)	95.06 (4.02)*	12.04 (0.64)*	2.93 (0.43)*	0.33 (0.06)*	0.084 (0.03)
P31 (6-10-60)	96.63 (3.00)*	11.62 (0.50)*	2.71 (0.21)*	0.36 (0.04)*	0.080 (0.03)
P32 (6-15-15)	81.59 (9.81)	13.70 (1.51)	3.44 (0.83)*	0.25 (0.06)	0.104 (0.03)
P33 (6-15-30)	91.51 (6.11)	12.80 (0.86)*	3.11 (0.71)*	0.31 (0.07)*	0.091 (0.02)
P34 (6-15-45)	95.08 (4.00)*	12.03 (0.63)*	2.93 (0.43)*	0.33 (0.06)*	0.084 (0.03)
P35 (6-15-60)	96.66 (2.98)*	11.62 (0.49)*	2.74 (0.25)*	0.35 (0.04)*	0.079 (0.03)

*Significantly different from the standard protocol (SP) ($P < .05$).
BHC, beam hardening correction; *BV/TV,* bone volume/total volume; *BS/TV,* bone surface/total volume; *RAC,* ring artifact correction; *SD,* standard deviation; *SF,* smoothing filter; *Tb.N;* trabecular number; *Tb.Th,* trabecular thickness; *Tb.Sp,* trabecular separation.

With regard to Tb.Sp, protocols P1, P2, P4, P5, P7, P8, P9, P11, P12, P13, P16, P17, P20, and P21 were different from the SP ($P < .05$) (see Table I). This means that in general, protocols with SF of 2 or 4 and BHC other than 45% were statistically different from the SP, except for P3 (SF of 2 and BHC at 60%). All protocols with SF of 6 were statistically similar to the SP (see Table I).

For DA, none of the tested protocols differed significantly from the SP ($P > .05$). For Conn.D, only P0 and protocols with SF at 2 and BHC at 15% were statistically different from the SP ($P < .05$); all other protocols were similar to the SP. For total porosity, with the exception of protocols P6 and P10 (SF at 2 and BHC at 45%) and protocols P13, P17, P21, P24, P25, P28, P29, P32, and P33 (SF at 4 and BHC at 30%, and SF at 6 and BHC at 15 or 30%), all the other protocols were statistically different from the SP ($P < .05$) (see Table II).

DISCUSSION

According to our findings, the BHC and SF algorithms are the most influential factors in micro-CT image reconstructions. BHC levels had an inverse or direct relationship with bone microarchitecture values. This can be attributed to the fact that the beam hardening phenomenon is inherent to the process of X-ray imaging, as the polychromatic radiation beam is filtered through the structures, resulting in an increase of its average energy until it reaches the image receptor.[12,13] This phenomenon can affect the accuracy of data

Table II. Mean values (SD) of degree of anisotropy, connectivity density, and total porosity for each micro-CT reconstruction protocol (SP and P0 to P35)

Protocols (SF-RAC-BHC)	*Microarchitecture parameters − Mean (SD)*		
	Degree of anisotropy (DA)	*Connectivity density (Conn.D)*	*Total porosity (Po-tot)*
SP (2-5-45)	2.616 (0.45)	105.207 (64.65)	8.951 (4.89)
P0 (0-0-0)	3.271 (1.09)	14474.985 (3136.85)*	54.493 (4.21)*
P1 (2-5-15)	3.077 (1.29)	320.585 (59.41)*	21.953 (7.36)*
P2 (2-5-30)	2.855 (0.62)	176.669 (96.71)	12.917 (6.10)*
P3 (2-5-60)	2.646 (0.64)	82.379 (68.37)	6.742 (4.11)*
P4 (2-10-15)	3.047 (1.28)	328.525 (69.95)*	21.939 (7.35)*
P5 (2-10-30)	2.822 (0.58)	176.668 (102.70)	12.881 (6.10)*
P6 (2-10-45)	2.614 (0.42)	103.222 (66.71)	8.908 (4.89)
P7 (2-10-60)	2.611 (0.60)	78.409 (60.72)	6.753 (4.08)*
P8 (2-15-15)	3.156 (1.41)	315.622 (63.12)*	21.951 (7.31)*
P9 (2-15-30)	2.789 (0.60)	172.699 (107.04)	12.861 (6.10)*
P10 (2-15-45)	2.605 (0.46)	120.095 (82.85)	8.881 (4.89)
P11 (2-15-60)	1.824 (1.24)	71.461 (60.54)	6.719 (4.06)*
P12 (4-5-15)	2.293 (0.60)	105.207 (26.35)	19.952 (8.70)*
P13 (4-5-30)	2.559 (0.50)	52.603 (26.40)	10.633 (6.21)
P14 (4-5-45)	2.463 (0.57)	30.766 (22.31)	6.840 (4.60)*
P15 (4-5-60)	2.279 (0.64)	22.828 (5.66)	4.890 (3.63)*
P16 (4-10-15)	2.296 (0.62)	104.215 (19.54)	19.914 (8.71)*
P17 (4-10-30)	2.542 (0.53)	48.633 (22.58)	10.583 (6.22)
P18 (4-10-45)	2.520 (0.63)	31.760 (24.96)	6.800 (4.60)*
P19 (4-10-60)	2.294 (0.67)	21.835 (4.44)	4.867 (3.62)*
P20 (4-15-15)	2.352 (0.66)	111.162 (23.95)	19.918 (8.70)*
P21 (4-15-30)	2.522 (0.54)	48.633 (20.28)	10.555 (6.23)
P22 (4-15-45)	2.534 (0.65)	38.708 (31.66)	6.766 (4.58)*
P23 (4-15-60)	2.282 (0.63)	23.820 (6.47)	4.846 (3.60)*
P24 (6-5-15)	2.469 (0.60)	43.671 (16.23)	18.464 (9.79)
P25 (6-5-30)	2.587 (0.82)	22.828 (17.05)	8.549 (6.12)
P26 (6-5-45)	2.391 (0.89)	6.947 (4.44)	4.960 (4.02)*
P27 (6-5-60)	2.243 (0.64)	7.940 (7.53)	3.387 (3.01)*
P28 (6-10-15)	2.410 (0.63)	45.655 (15.05)	18.424 (9.81)
P29 (6-10-30)	2.521 (0.75)	24.813 (18.23)	8.515 (6.12)
P30 (6-10-45)	2.360 (0.88)	7.940 (4.44)	4.939 (4.02)*
P31 (6-10-60)	2.258 (0.68)	7.940 (7.53)	3.366 (3.00)*
P32 (6-15-15)	2.444 (0.73)	46.648 (13.41)	18.412 (9.81)
P33 (6-15-30)	2.480 (0.64)	24.813 (18.23)	8.487 (6.11)
P34 (6-15-45)	2.392 (0.93)	10.917 (7.36)	4.922 (4.00)*
P35 (6-15-60)	2.263 (0.61)	8.932 (7.36)	3.339 (2.98)*

*Significantly different from the standard protocol (SP) ($P < .05$).
BHC, beam hardening correction; *RAC,* ring artifact correction; *SD,* standard deviation; *SF,* smoothing filter.

obtained and, consequently, the qualitative and quantitative analyses.[4]

Bone microarchitecture parameters were affected in different ways with application of the BHC tool. As its level of application increased, BV/TV and Tb.Th values increased, whereas the value of the other parameters decreased. As no previous report has investigated the effect of reconstruction protocols on these parameters, comparing this result with other published data becomes difficult. However, other studies evaluating bone structure with the use of different methods or acquisition parameters[14,15] also demonstrated an inverse relationship between BV/TV and Tb.Th values and other microarchitecture parameters. This relationship is expected because such parameters correspond to the inversely proportional characteristics of bone tissue and are determined by interdependent 3-D calculations[5]; for example, the greater the trabeculae thickness (Tb.Th), the smaller is the spacing between them (Tb.Sp).

SF acts to reduce the noise of the entire image,[9] and this may be related to its effect on bone microarchitecture analysis. In general, increased SF levels combined with BHC reduction maintained bone microarchitecture values similar to those in the SP.

According to the literature,[16] the function of the RAC tool is to correct artifacts caused by uncalibrated or defective detector elements, which are visible as dark or bright circles around the center of rotation within a micro-CT slice. In the present study, the different RAC settings did not affect the values of bone

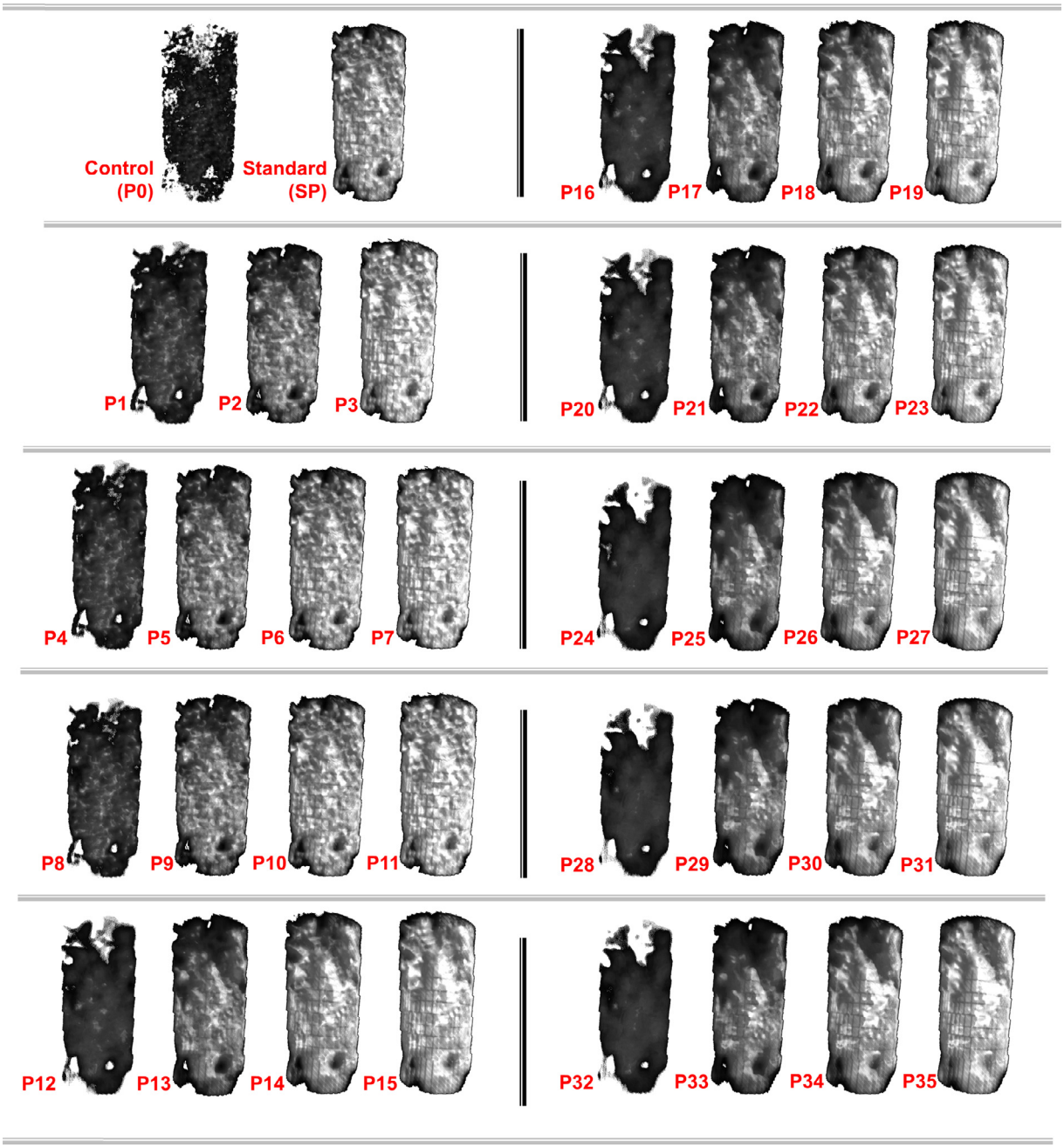

Fig. 1. Three-dimensional (3-D) reconstruction of the volume of interest assessed for the bone microarchitecture analysis in the control protocol (P0), the standard protocol (SP), and protocols P1 to P35.

microarchitecture parameters, probably because a calibrated micro-CT unit was used and ring artifacts were not present in the images. However, it was necessary to test the RAC tool to make sure that it did not have any negative influence on the images that had no ring artifacts to be corrected.

DA, which represents a description of how the structural elements are oriented,[5,17] was the only microarchitectural parameter that was not significantly affected by any of the artifact correction tools. We believe this result occurred because in the samples used in this project, beam hardening and noise artefacts did not affect the detection of trabecular spatial orientation. However, Po-tot and Conn.D were inversely affected by BHC and SF. These parameters are also related to structural strength and indicate the relationship between the number of open and closed pores and the degree to which parts of the object are connected in multiple ways,[17] respectively.

Aside from Tb.Sp and DA, the control protocol (P0) presented values significantly different from those in

Table III. Morphometric parameters analyzed, with their symbols, descriptions, and units of measurement*

Morphometric parameter	*Abbreviation*	*Description*	*Unit*
Percent bone volume	BV/TV	Proportion of bone occupying the volume of interest (VOI)	%
Bone surface density	BS/TV	Ratio of bone surface within the VOI—characterizes the structure complexity and thickness	mm^{-1}
Trabecular number	Tb.N	Number of transversals across a structure	mm^{-1}
Trabecular thickness	Tb.Th	Average thickness of trabecular structure according to a sphere-fitting method	mm
Trabecular separation	Tb.Sp	Average thickness of empty spaces in a trabecular structure according to the sphere-fitting methods	mm
Degree of anisotropy	DA	Alignment of the structures along a directional axis.	None
Connectivity density	Conn.D	Number of connections between trabecular structures	mm^{-3}
Total porosity	Po(tot)	Percent of all open and closed pores within the VOI	%

*According to Bruker-Micro-CT Analyser: Morphometric parameters on 3-dimensional (3-D) and 2-dimensional (2-D) images.[11]

the SP in the analysis of all other parameters of bone microarchitecture. This result highlights the magnitude of the influence of artifacts on micro-CT images when no artifact correction tool is applied and reveals the importance of using the BHC and SF tools during the reconstruction process. Although not demonstrated in this investigation, the RAC tool may also be helpful if the scanner is not properly calibrated.

Morphometric indices are the standard method to quantitatively characterize bone architecture. The essential series of variables that should be stated for trabecular bone includes BV/TV, Tb.Th, Tb.Sp, and Tb.N, to allow for comparison with classic histomorphometry studies. Moreover, subject to the fundamental core of a research study, variables based on 3-D calculations can be reported.[5] The present study analyzed all of these parameters, showing that both 2-D and 3-D variables are affected by the reconstruction parameters.

Although the rat maxilla has an architecture similar to that of human bone, results should not be directly extrapolated to humans because the size and density of rat trabeculae are different from human trabeculae and this may cause artifacts of different magnitudes. Future studies should explore the influence of artifact correction tools on the reconstruction of human bone specimens and cortical and long bones.[5] To avoid partial-volume effects and overestimation of object thickness, voxels smaller than the thickness of the analyzed structure must be used. In the present study, a voxel size of 10.2 μm was used. This allowed for distinction of the trabeculae, which range in size from 20 to 60 μm.[2,5] In addition, a single threshold was used for all scans, ensuring that the differences between protocols resulted from reconstruction parameter effects rather than from image-processing effects.

CONCLUSIONS

Bone microarchitecture parameters are influenced by the levels of the artifact correction tools applied, mainly by BHC and SF. In general, increased SF levels combined with BHC reduction maintain the values of the microarchitectural parameters, as in the SP. In future studies, standardization and clear specification of those levels are necessary to allow for correct interpretation and comparisons of results.

FUNDING

This study was financed, in part, by the Coordenação de Aperfeiçoamento de Pessoal de Nível Superior, Brazil (CAPES) (Finance Code 001).

REFERENCES

1. Suttapreyasri S, Suapear P, Leepong N. The accuracy of cone-beam computed tomography for evaluating bone density and cortical bone thickness at the implant site. *J Craniofac Surg*. 2018;00:1.
2. Ruegsegger P, Koller B, Muller R. A microtomographic system for the nondestructive evaluation of bone architecture. *Calcif Tissue Int*. 1996;58:24-29.
3. González-García R, Monje F. Is micro-computed tomography reliable to determine the microstructure of the maxillary alveolar bone? *Clin Oral Implants Res*. 2013;24:730-737.
4. Koubar K, Bekaert V, Brasse D, Laquerriere P. A fast experimental beam hardening correction method for accurate bone mineral measurements in 3 D μCT imaging system. *J Microsc*. 2015;258:241-252.
5. Bouxsein ML, Boyd SK, Christiansen BA, Guldberg RE, Jepsen KJ, Müller R. Guidelines for assessment of bone microstructure in rodents using micro-computed tomography. *J Bone Miner Res*. 2010;25:1468-1486.
6. Campbell GM, Sophocleous A. Quantitative analysis of bone and soft tissue by micro-computed tomography: applications to ex vivo and in vivo studies. *Bonekey Rep*. 2014;3:1-12.
7. Kyriakou Y, Prell D, Kalender WA. Ring artifact correction for high-resolution micro CT. *Phys Med Biol*. 2009;54:N385-N391.
8. Zhu Y, Zhao M, Li H, Zhang P. Micro-CT artifacts reduction based on detector random shifting and fast data in painting. *Med Phys*. 2013;40:031114.
9. Irie MS, Rabelo GD, Spin-Neto R, Dechichi P, Borges JS, Soares PBF. Use of micro-computed tomography for bone evaluation in dentistry. *Braz Dent J*. 2018;29:227-238.
10. Peyrin F, Dong P, Pacureanu A, Langer M. Micro- and nano-CT for the study of bone ultrastructure. *Curr Osteoporos Rep*. 2014;12:465-474.

11. Bruker-micro CT. Morphometric parameters measured by Skyscan CT - Analyser software. *Ref Man*. 2012;1:1-30. Available at: https://medicine.temple.edu/sites/medicine/files/files/ct_analyzer.pdf.
12. Mulder L, Koolstra JH, Van Eijden TMGJ. Accuracy of microCT in the quantitative determination of the degree and distribution of mineralization in developing bone. *Acta Radiol*. 2004;45:769-777.
13. Meganck JA, Kozloff KM, Thornton MM, Broski SM, Goldstein SA. Beam hardening artifacts in micro-computed tomography scanning can be reduced by X-ray beam filtration and the resulting images can be used to accurately measure BMD. *Bone*. 2009;45:1104-1116.
14. Van Dessel J, Nicolielo LFP, Huang Y, et al. Accuracy and reliability of different cone beam computed tomography (CBCT) devices for structural analysis of alveolar bone in comparison with multislice CT and micro-CT. *Eur J Oral Implantol*. 2017;10:95-105.
15. Van Dessel J, Huang Y, Depypere M, Rubira-Bullen I, Maes F, Jacobs R. A comparative evaluation of cone beam CT and micro-CT on trabecular bone structures in the human mandible. *Dentomaxillofacial Radiol*. 2013;42:20130145.
16. Scherf H, Tilgner R. A new high-resolution computed tomography (CT) segmentation method for trabecular bone architectural analysis. *Am J Phys Anthropol*. 2009;140:39-51.
17. Odgaard A. Three-dimensional methods for quantification of cancellous bone architecture. *Bone*. 1997;20:315-328.

Reprint requests:

Eduarda Helena Leandro Nascimento
Department of Oral Diagnosis
Piracicaba Dental School
University of Campinas
Av. Limeira, 901
Zip Code 13414-903
Piracicaba
Sao Paulo
Brazil.
eduarda.hln@gmail.com